Prevalence of Precipitation from Warm-Topped Clouds over Eastern Asia and the Western Pacific

GRANT W. PETTY

Department of Earth and Atmospheric Sciences, Purdue University, West Lafayette, Indiana

(Manuscript received 9 June 1997, in final form 16 February 1998)

ABSTRACT

Land and ship surface synoptic reports of nondrizzle intensity precipitation in progress were matched with 3596 nearly coincident full disk 4-km resolution infrared images from the *GMS-5* geostationary satellite, covering 18 calendar months, in order to derive regional and seasonal estimates of the contribution of relatively warm-topped clouds to the total time in precipitation.

Minimum infrared temperatures of 273 K or warmer were found to be associated with 20%–40% of the surface reports of nondrizzle precipitation over much of the ocean east of Australia during all four seasons. Similar or even larger fractions were found during December–March over parts of Indochina, southern China, and the adjacent South China Sea. Although reports of precipitation of moderate or heavy intensity were found to be associated more often with colder cloud tops, there were still regions for which a substantial fraction of these reports were associated with relatively warm clouds. These results suggest at least a potential for significant regional and seasonal biases in satellite infrared or passive microwave scattering based estimates of global precipitation.

1. Introduction

Many widely used satellite techniques for estimating precipitation rely on either infrared (IR) observations of very cold cloud-top temperatures or passive microwave (PMW) observations of scattering by frozen precipitation aloft (see reviews by Arkin and Ardanuy 1989; Petty 1995a; Petty and Krajewski 1996). Both classes of algorithms therefore detect mainly precipitation associated with cold, often deep convective rain clouds, while overlooking precipitation contributed by shallower clouds with warm IR tops and little or no ice.

Unfortunately, the otherwise attractive alternative of techniques utilizing microwave emission or attenuation information (e.g., Wilheit et al. 1991; Liu and Curry 1992; Bauer and Schluessel 1993; Petty 1994a,b), which is more directly related to near-surface liquid precipitation, can be employed only over ocean areas. Therefore, IR and scattering-based PMW algorithms, which can be used over both land and water, have come to play an important role in the generation of global precipitation products—for example, gridded monthly rainfall totals, such as those disseminated by the Global Precipitation Climatology Project (Huffman et al. 1997) and other laboratories (Adler et al. 1994; Xie and Arkin 1996; Ferraro et al. 1996).

In the absence of better information, an implicit assumption in the generation of global rainfall products from satellite data has been that the relative contribution of warm rain to precipitation totals at locations around the world is small, or at least approximately constant, and that this ''silent'' warm rain contribution is accounted for automatically when algorithms are empirically calibrated over long time periods against surface validation data at a few locations. To date, however, there has never been a climate-scale survey of the actual occurrence of rain from warmer clouds, using reasonably unambiguous and homogeneous data sources. The true magnitude of the warm rain contribution to total rainfall and, particularly, of its regional and seasonal variability remains a matter of conjecture. It has therefore been difficult to assess the potential for regional and seasonal biases in the satellite-derived precipitation products now finding extensive use in climate and hydrological studies.

However, Janowiak et al. (1995) showed that different remote sensing techniques lead not only to significant differences in estimated rainfall amounts in the east Pacific intertropical convergence zone but even to differences in the sign of the zonal rainfall gradient. This finding apparently reflects the differing responses of each satellite technique to regional variations in the microphysical properties of rain clouds.

Corresponding author address: Dr. Grant W. Petty, Purdue University, Department of Earth and Atmospheric Sciences, 1397 Civil Engineering Building, West Lafayette, IN 47907-1397.
E-mail: gpetty@purdue.edu

Although it has long been known that rainfall from warm clouds, especially trade wind cumulus congestus over the ocean, is not rare (e.g., Battan and Braham 1956), there have been few attempts to estimate its climatological prevalence on regional and seasonal scales, presumably owing to a lack of suitable observations. In one of the most recent such studies, Liu et al. (1995) analyzed coincident satellite microwave rain rate estimates and infrared cloud-top temperatures in the western equatorial Pacific for November 1992 through February 1993. They concluded that clouds with tops warmer than 273 K contributed approximately 14% to the total time–area-weighted occurrence of rain, and approximately 9% to the total rainfall accumulation in that region. They also acknowledged that these figures might err on the low side on account of the presumed inability of the microwave instrument to resolve rainfall from scattered cumulus congestus clouds, a concern that appears to be corroborated by a validation study undertaken by Petty (1997). Some other studies that have discussed the prevalence and/or properties of precipitation from relatively warm clouds, primarily over the tropical and subtropical oceans, include Woodley (1980), Augustine (1981), Szoke and Zipser (1986), Takahashi and Uyeda (1995), Williams et al. (1995), and Sui et al. (1997).

This paper presents what is believed to be the first superregional and multiseasonal analysis of the time-weighted fractional occurrence of surface rainfall from clouds with relatively warm tops, based on 18 months of full disk 3-hourly IR images matched with surface synoptic reports of precipitation in progress. For this initial analysis, data from the Japanese *GMS-5* satellite are employed, which limits the geographic coverage to much of the western Pacific and eastern Asia. The details of the geographic coverage are further constrained by the availability of coincident surface reports of precipitation, a factor that unfortunately eliminates the Australian continent and some less heavily trafficked ocean areas from consideration.

Owing to the qualitative nature of the synoptic present weather reports used in this analysis (rain gauge reports with adequate geographic density and time resolution are not readily available), the present analysis cannot be used to infer the relative contribution of warm-topped clouds to precipitation *amount* at a location. Nevertheless, where atypical contributions of warm rain to total *time in precipitation* (TIP) are noted, such a finding suggests the possibility of an atypical contribution of warm clouds to the rainfall amount at that location as well, especially if the anomaly exists for precipitation events classified as ''moderate or heavy'' in intensity.

2. Data and methods

The *GMS-5* geostationary satellite is positioned over the equator at approximately 140°E long and provides coverage of Australia, East Asia, and Japan, and the western Pacific Ocean. Full disk digital IR images at 4-km resolution and 3-h intervals were obtained in hierarchical data format from mid-1995 through spring 1997. The data files include accurate navigation information for the geographic area within a 50° angular radius of the satellite subpoint.

Global surface synoptic reports, including both ship and land stations, were obtained for the same period of time. The primary reported element of interest for this study is the two-digit present weather code (ww), which encodes subjective observations of the weather affecting the station at the time of the observation or during the hour preceding the observation. Most of the 99 available codes describe obstructions to visibility (e.g., fog, haze, blowing dust, sand, or snow), thunderstorms, and/or precipitation classified by phase, intensity, and character (e.g., showers vs steady precipitation). See Petty (1995b) for additional information concerning the definitions of the present weather codes relevant to precipitation and for a discussion of some of the ambiguities in their interpretation.

GMS image scans typically begin some 27 minutes prior to each hour, but the scanning process requires several minutes to complete, so a given location will actually be observed somewhat later than the nominal image time, depending on latitude. Similarly, although nominal synoptic reporting times are exact multiples of 3 hours, the actual observations, including determination of present weather, usually begin ~15 minutes prior to the hour. In view of both practices, the actual time separation between a GMS image for, for example, 0233 UTC and the corresponding surface synoptic observation at 0300 UTC is usually less than 15 minutes.

All available surface synoptic reports from standard 3-hourly reporting times and within the region covered by the *GMS-5* satellite were matched with the corresponding full-disk IR image, when available. The relevant content of the report was then saved along with the 5×5 array of IR pixels centered on the synoptic station. The sample was further restricted for this study to synoptic reports giving a positive indication of surface precipitation at or near the station at the time of the observation. Present weather code 14, indicating virga (precipitation not reaching the surface), was excluded from the sample.

The precipitation observations were further classified according to the qualitative intensity of the precipitation and as to whether the precipitation directly affected the station at the time of the observation or rather was observed reaching the surface at some distance from the station. When precipitation does fall at the station, the available present weather codes generally permit a distinction to be made between 1) drizzle-intensity precipitation (i.e., very small water drops or snow grains), which rarely gives rise to measurable accumulations; 2) precipitation that is ''slight,'' generally implying the presence of bona fide raindrops or snowflakes, but with accumulation rates less than a nominal threshold of 2.5

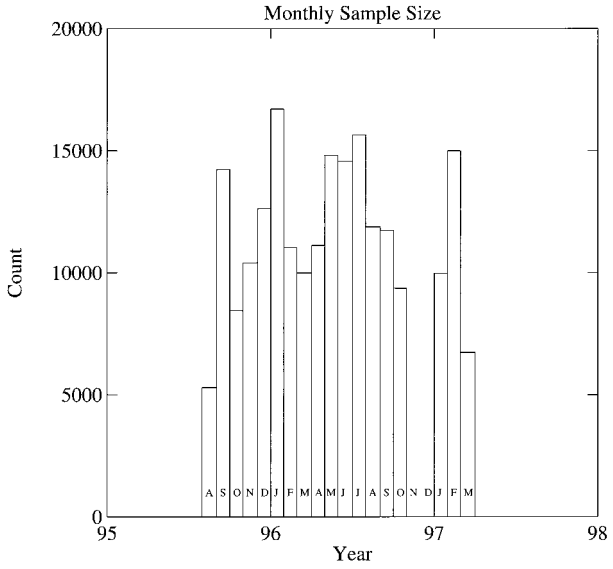

FIG. 1. Number of matchups of nondrizzle-intensity surface precipitation events and *GMS-5* brightness temperatures for each month in the study period.

mm h^{-1}; and 3) precipitation that is ''moderate or heavy'' at the time of the observations, implying estimated accumulation rates greater than 2.5 mm h^{-1} (Petty 1995b). Although the presence or absence of precipitation can be determined with a high degree of reliability by a surface observer, the assessment of intensity class is usually subjective and is therefore unreliable as a basis for assigning an actual precipitation rate. Moreover, the classification ''moderate or heavy'' encompasses an extremely broad range of possible precipitation rates.

The final matchup dataset was derived from a total of 3596 full-disk satellite images. The total number of usable synoptic reports of nondrizzle intensity precipitation in progress was approximately 2.1×10^5. The monthly distribution of point matchups satisfying this intensity criterion is depicted in Fig. 1. Variations in the sample size could reflect any of the following factors: 1) gaps in the local *GMS-5* archive, 2) gaps in the local synoptic archive, and/or 3) variations in the total number of synoptic stations affected by precipitation in a given month.

When drizzle-intensity precipitation is included (not shown), the number of matchups increases by approximately 10%–20%, depending on location. If, on the other hand, the sample is limited to precipitation of moderate or heavy intensity, the sample is typically reduced by a factor of 2 or more. Finally, the inclusion of precipitation seen near but not at the station at the time of the observation (the most common single category of precipitation report over the ocean; Petty 1995b) increases the sample size by up to a factor of 2 or more over the ocean, but only slightly over most land areas.

The matched data were then stratified into 3-month seasons and 5° lat × 5° long bins. Figure 2 depicts the geographic distribution of the sample size for local, nondrizzle precipitation for each season. Over much of East Asia, the sample density is quite high, with well over 300 satellite-matched reports of per season per grid box. Over other areas, the density is much lower, either due to a general scarcity of synoptic reports, as is the case over the eastern portion of the tropical Pacific Ocean, or in some cases owing to the relative rarity of precipitation.

The Australian landmass coincides with an unfortunate hole in the coverage by this matchup set due to that nation's practice of submitting synoptic reports at nonstandard times. Since GMS imagery was retained in the Purdue archive only for multiples of 3 hours, the Australian reports could not be used for this study.

From each set of 25 IR pixels matched to a surface synoptic report, the minimum IR brightness temperature was determined. This value thus represents the coldest 4-km-average cloud-top temperature observed within a 10–15-km radius of a station that is reporting nearly simultaneous surface precipitation.

There are two significant ambiguities in interpretation of the IR brightness temperature statistics that should be kept in mind throughout the rest of this paper. First, it is possible for a higher, nonprecipitating cloud layer (e.g., cirrus) to reduce the IR brightness temperature relative to the temperature of the top of the cloud that is actually producing precipitation. Second, subpixel variability of cloud-top temperature, such as might be associated with localized convective showers, may lead to an overestimate of the minimum cloud-top temperature associated with a precipitation event. Both ambiguities are of concern only when attempting a cloud physical interpretation of the analysis results, as opposed to merely assessing the potential for biases in IR-derived rainfall estimates.

Additional errors could arise from larger-than-expected image navigation errors or from rapid changes in cloudiness within 10+ km of the station during the 10–15 minutes elapsing between image time and the surface observation. Systematic errors due to these problems are most likely to be significant for stations whose precipitation is dominated by transient, isolated convective showers.

3. Results

Figures 3–5 depict the fraction of selected surface precipitation reports for which minimum IR brightness temperatures, as defined above, were warmer than 273, 268, 263, and 253 K (panels a–d, respectively, in Figs. 3–5), for each season. Fractions were computed only for grid boxes in which at least 10 qualifying reports, with matching IR data, were available. Grid boxes not satisfying this minimal requirement are not plotted. In generating the seasonal statistics, no attempt was made to correct for unevenly distributed monthly sample sizes

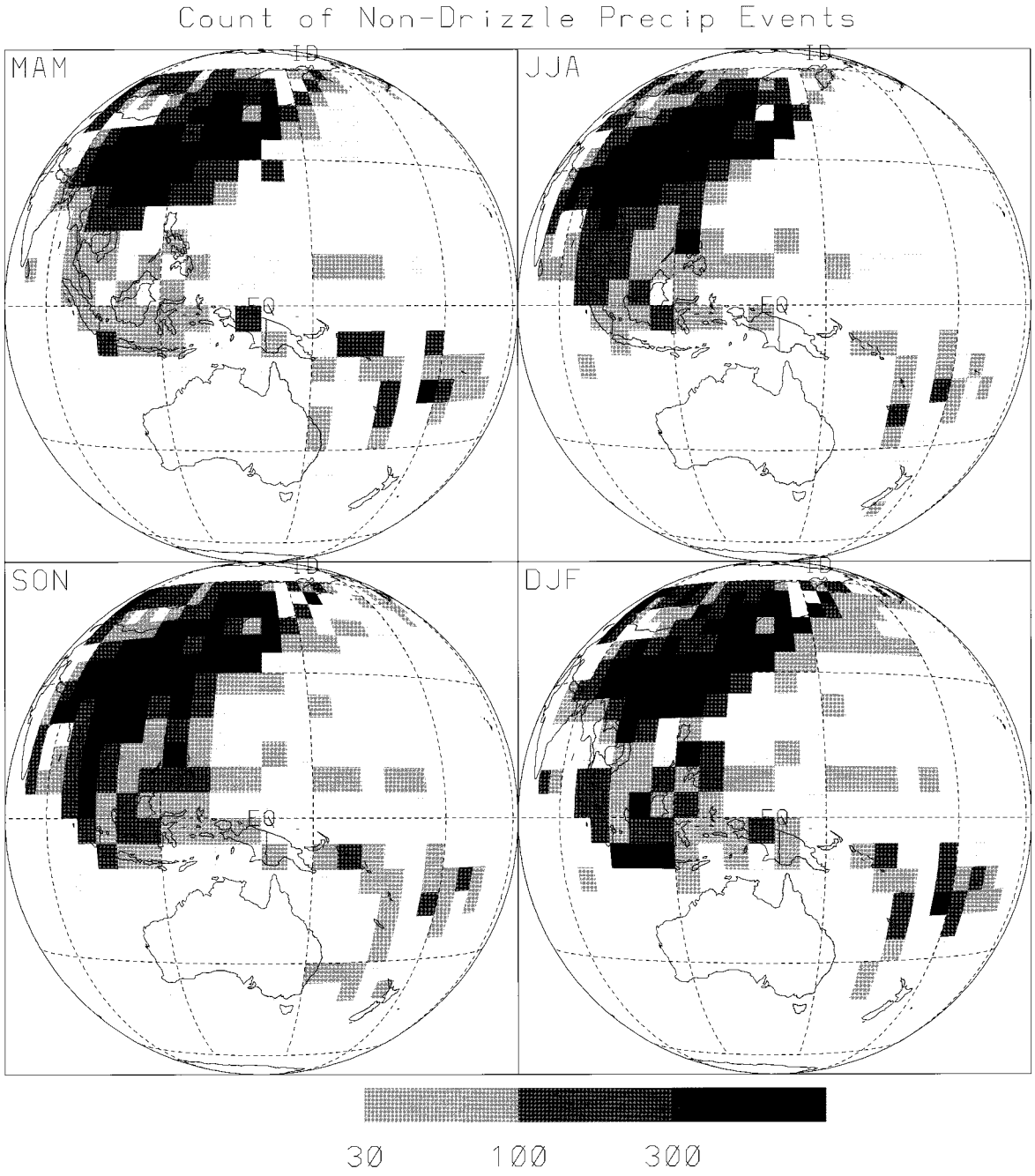

FIG. 2. For each 5° grid box, the number of available surface synoptic reports in the study sample indicating nondrizzle-intensity precipitation in progress at the station. Only grid boxes for which the number is at least 10 are plotted: (a) Mar–M (b) Jun–Jul, (c) Sep–Nov, (d) Dec–Feb.

or for unbalanced contributions from each of the years 1995–97.

The minimum sample size of 10 reports is based on a subjective optimization of the trade-off between geographic coverage and statistical robustness. When the available sample approaches this minimum value, there will be occasional statistical ''flukes'' in which the computed fraction is much larger or smaller than the true long-term average fraction. For small samples, the best qualitative indication of the reliability of the computed fractions at a location is the degree of coherence in space since sampling-related errors in one grid box will be statistically uncorrelated with those in neighboring grid boxes.

For Fig. 3, the sample includes not only all forms of precipitation directly affecting the station at the time of

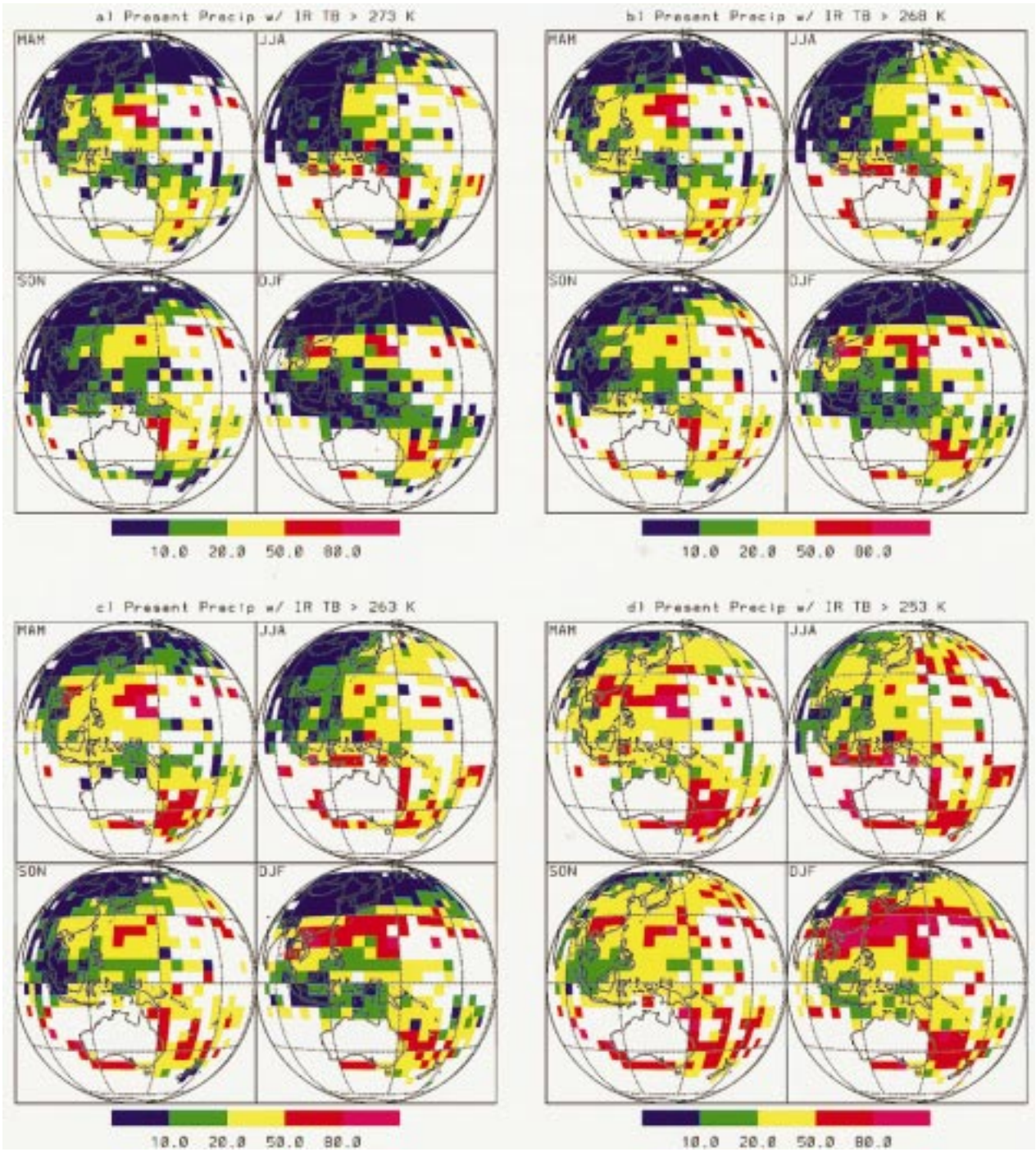

FIG. 3. For each 5° grid box, the percentage of surface reports of precipitation observed at or near the station at the time of the observation for which the minimum coincident satellite IR brightness temperature was warmer than the indicated threshold: (a) 273 K, (b) 268 K, (c) 263 K, and (d) 253 K.

the observations, but also all reports of precipitation reaching the surface within sight of the station (groups 1, 7, 10–12, and 14–31 according to Table 3 of Petty 1995b). Under these conditions, a large portion of the western Pacific Ocean and virtually all of eastern Asia yield an adequate sample of surface–satellite matchups.

Over most of the ocean, 10%–50% of qualifying precipitation reports are found to be associated with IR brightness temperature minima warmer than 273 K, whereas a much smaller fraction over land satisfy this condition. This result is generally consistent with Battan and Braham (1956), who observed that warm-topped

maritime convective clouds precipitate far more readily than continental clouds of similar depth. Indeed, over the Caribbean Sea, they found that 50% of all cumulus clouds reaching the +6°C isotherm exhibited radar echoes, and no cloud reaching the freezing level failed to exhibit an echo.

As an (imperfect) estimate of cloud-top temperature, the IR threshold of 273 K is particularly significant because it represents the conventional dividing line between cold clouds, that is, those for which ice processes may contribute to precipitation formation, and warm clouds, in which ice cannot be present and from which all precipitation must be produced solely by collision/coalescence of liquid droplets. A rain cloud whose top is warmer than 273 K will not only fail to be detected by most IR-based algorithms, but it will also be missed by any PMW technique which depends on the presence of frozen precipitation (graupel, snowflakes, hail, etc.) aloft.

Over most of Asia and the Maritime Continent, and over the northernmost Pacific Ocean, a far smaller fraction of qualifying precipitation reports is associated with warm IR cloud tops. There is a strong seasonal dependence in the frequency of precipitation from warmer clouds over the ocean north of 30°N lat the minimum occurring in December–February (DJF) and the maximum occurring in June–August (JJA). A comparable seasonal cycle occurs over and near the East Indies, though with a March–May (MAM) maximum immediately following the DJF minimum.

The DJF season is remarkable on account of a particularly pronounced belt of ''warm'' precipitation over southern China and over the ocean between approximately 15°N and 30°N. Within this belt, more than 50% of qualifying reports are associated with IR temperatures warmer than 263 K. The fraction increases to more than 80% for an IR threshold of 253 K.

Although Fig. 3 strongly suggests an important role for warm-cloud precipitation over the ocean, it must be recalled that the surface reports on which it is based include a large number of observations of precipitation within sight of, but not at, the station at the time of the observation. The statistics are therefore biased toward IR matchups with isolated showers, which may often be visible at some distance from a particular geographic point but which contribute only small amounts to the actual *time in precipitation* (TIP) at that point.

To obtain more realistic estimates of the fractional contribution of warm clouds to the total TIP, reports of nonlocal precipitation should be excluded from consideration. One may further exclude reports of precipitation of drizzle intensity since true drizzle rarely produces measurable accumulations at most locations and is therefore of limited hydrological interest.

Figure 4 is derived from reports of nondrizzle precipitation directly affecting the station at the time of the observation and of at least slight or greater intensity, that is, groups 7 and 14–31 according to Petty (1995b). Likewise, the statistics in Fig. 5 are based on surface reports of local precipitation of moderate or heavy intensity only, that is, groups 23–31. Because each figure in turn is based on a smaller sample, geographic coverage is progressively lost as local sample sizes fall below the threshold of 10 qualifying reports.

Figure 4 shows that the percentage of qualifying reports associated with warm clouds is significantly reduced by eliminating nonlocal precipitation (the elimination of drizzle-intensity reports is not responsible for most of the difference because they constituted a small fraction of the total). Throughout most of Asia, the North Pacific, and the deep Tropics, 80%–90% or more (as a fraction of TIP) of all nondrizzle precipitation is associated with IR temperatures colder than 263 K. Notable exceptions include the ocean areas east of Australia and between approximately 15° and 30°N lat, where as much as 20%–50% of TIP is associated with IR temperatures warmer than 273 K during the DJF season. Over and near southern China during this season, more than one-half of the total TIP is associated with IR temperatures warmer than 263 K, and fully 80% or more is associated with temperatures warmer than 253 K. Note that the latter fractions were computed from samples exceeding 300 reports, according to Fig. 2, therefore sampling uncertainties are small.

Although the results depicted in Fig. 4 clearly reveal regions of the western and southern Pacific and eastern Asia within which rain from comparatively warm clouds contributes up to 50% or more to total TIP, warm rain is expected to be lighter in intensity, on average, than rain from deeper clouds. Therefore the contribution of warm rain to total precipitation accumulation is expected to be smaller than its contribution to TIP.

Some indication of this tendency may be found in Fig. 5, in which the sample is restricted to reports of moderate or heavy precipitation affecting the station at the time of the observation. Over most areas for which an adequate sample is still available, there is a significant reduction, relative to Fig. 4, in the fraction of reports associated with IR temperatures warmer than any given threshold. This is particularly apparent for a threshold of 253 K (Figs. 4d and 5d), where typical fractions over eastern Asia drop from 20% to 50% for nondrizzle precipitation to less than 10% for moderate to heavy precipitation. The most notable exceptions are again east of Australia and over the South China Sea during some seasons, especially DJF, when approximately one-third of the moderate/heavy reports are associated with IR temperatures warmer than 273 K. More than 80% of these reports are associated with temperatures warmer than 253 K in the vicinitiy of Taiwan and southern China during DJF.

4. Discussion and conclusions

The statistical analysis of matched surface synoptic reports of precipitation and nearly simultaneous *GMS-5* full-disk IR images confirms that rainfall from rela-

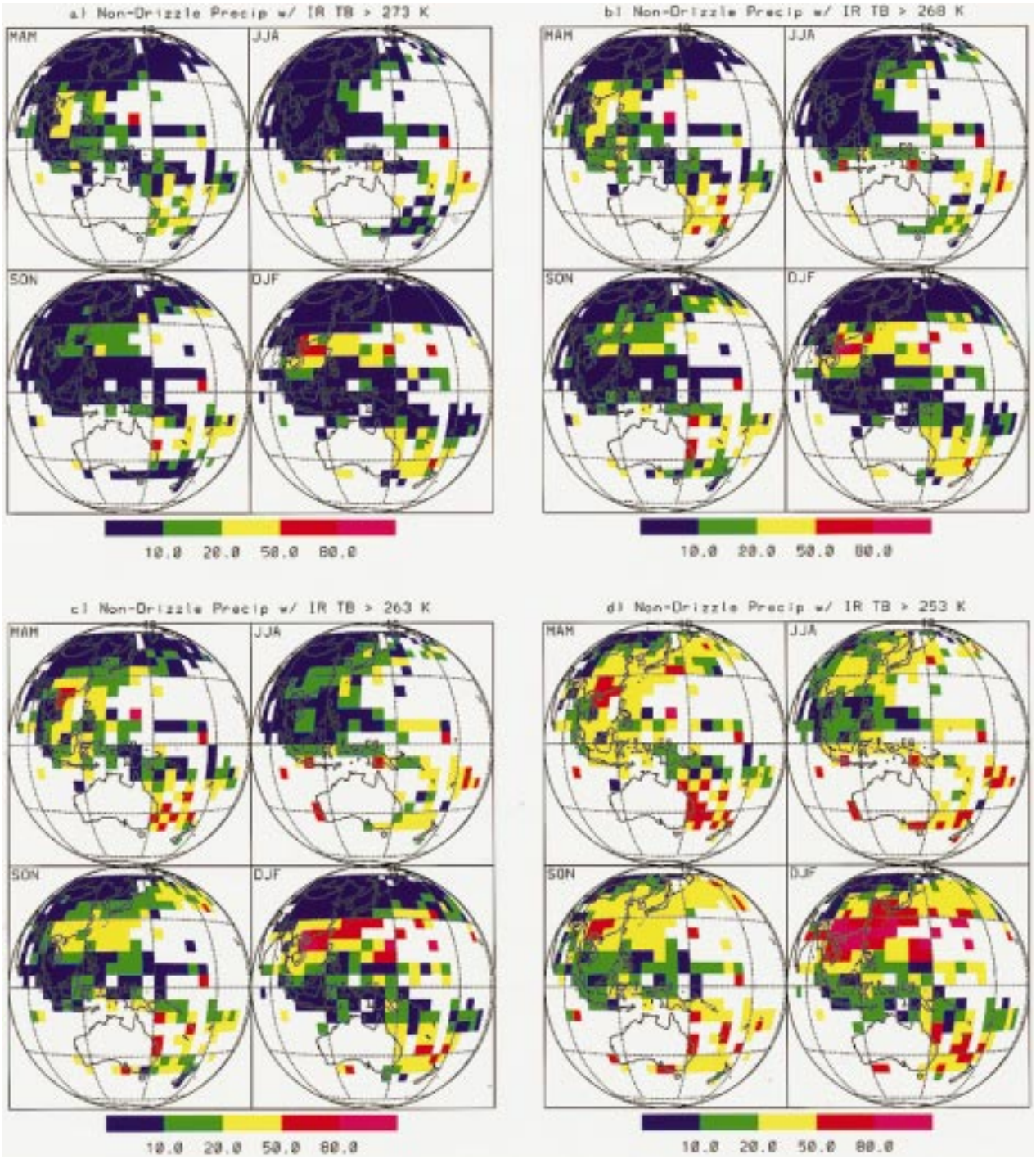

FIG. 4. As in Fig. 3 but utilizing only surface reports of precipitation of nondrizzle intensity directly affecting the station at the time of the observation.

tively warm clouds is not uncommon in some of the regions observed by this satellite. This finding suggests at least the possibility of significant regional and seasonal biases in satellite rainfall estimates based on algorithms and sensors sensitive primarily to cold-topped clouds. Although IR algorithms, in particular, partially compensate for missed warm rain by incorrectly classifying some nonprecipitating cirrus as rain, there is no reason to expect the degree of compensation to remain constant as one moves from regions dominated by deep, cold convection to regions affected primarily by trade wind cumulus showers.

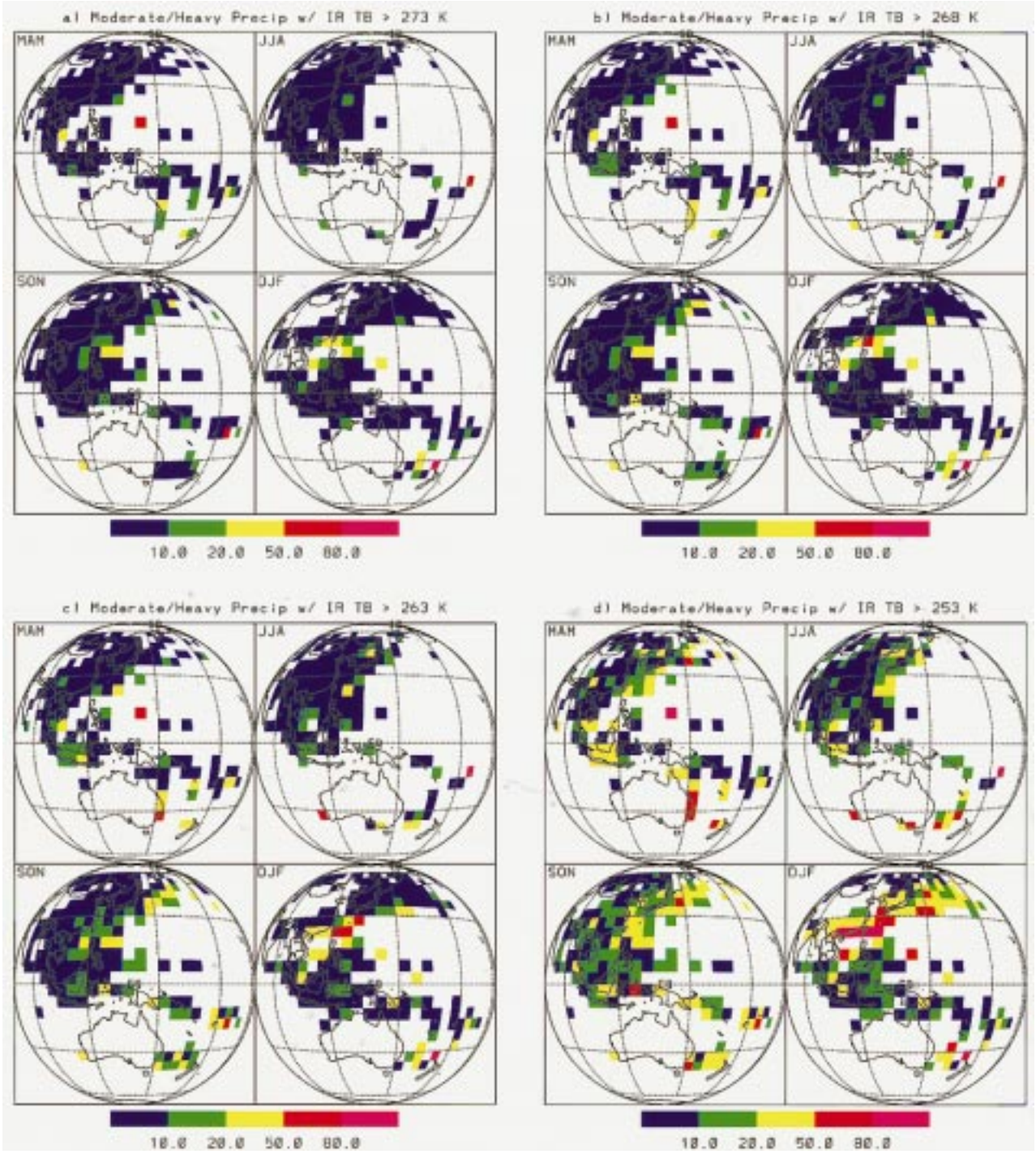

FIG. 5. As in Fig. 3 but utilizing only surface reports of precipitation of moderate or heavy intensity directly affecting the station at the time of the observation.

It must be emphasized that the statistics presented here describe the apparent contribution of relatively warm-topped clouds to the total TIP at a location, not necessarily to the total rainfall. If, as expected, cold-topped clouds usually precipitate more prodigiously than warm-topped clouds, then warm-topped clouds could contribute a large portion of the total TIP while contributing only a small fraction of the total rainfall accumulation. In such cases, the tendency for satellite algorithms to overlook warm rain may be of minor im-

portance. However, Fig. 5 revealed that there are a few regions in which even moderate to heavy precipitation is frequently associated with warm clouds.

One widely used IR rainfall estimation technique, the GOES Precipitation Index (GPI; Arkin and Meisner 1987; Arkin et al. 1994), employs a 235 K threshold for classifying a cloud as precipitating. During the recent 3D Precipitation Intercomparison Project (PIP-3), a number of satellite rainfall algorithms, including the GPI, were evaluated against surface validation data and against independent climatologies for an entire calendar year. Over large regions of the subtropical trade belts over ocean, the GPI estimated 250–500 mm less precipitation than is depicted for the same regions by the climatology of Jaeger (1983). Similar large differences were noted for many PMW algorithms, especially those relying heavily on the 85.5-GHz ice scattering signature for the detection of precipitation. Over other regions, such as the ITCZ, the satellite algorithms tended to find more precipitation than the climatology. Although the accuracy of the Jaeger climatology over the regions in question is quite uncertain, it is nevertheless intriguing that the patterns of differences between satellite and climatology agree well with the patterns of greater and lesser fractional contributions by warm-topped clouds, as determined here.

Several obvious avenues for further research can be identified. Among other things, it would be useful to enlarge the statistical sample for the regions considered in this study by employing a longer time series of *GMS-5* imagery. Including images from times matching the Australian synoptic reporting schedule would permit an important hole in the current analysis to be filled. Including satellite images from the American Geostationary Operational Environmental Satellite (GOES) and European Meteosat satellites would allow the geographic coverage of this analysis to be extended to most of the Western Hemisphere.

All of the above enhancements are contingent on the availability, at a reasonable cost, of a sufficiently long time series of digital imagery from the respective sensors. Currently, large orders for retrospective geostationary satellite data through normal channels are either prohibitively expensive (e.g., discounted price $120 000 per satellite-year for 3-hourly GOES images from the National Climate Data Center) or else are simply unmanageable logistically from the perspective of the responsible data center. Although it might be thought that the data products of the International Satellite Cloud Climatology Project could help overcome this difficulty, note that these products could not have been used for the present analysis, owing to their inadequate temporal precision (± 1.5 h) for the purpose of matching satellite data to surface synoptic reports.

On the other hand, the recently launched Tropical Rainfall Measuring Mission (TRMM; Simpson et al. 1996) carries the first satellite-borne precipitation radar (PR), as well as a visible infrared scanner, and a TRMM Microwave Imager. The PR will provide an unambiguous indication of the presence of precipitation under warm-topped clouds equatorward of approximately 38° lat. Combining information from all three instruments will allow regional characteristics of tropical and subtropical precipitation to be determined with unprecedented detail and precision.

Acknowledgments. *GMS-5* images were obtained in near real time via anonymous ftp from the Department of Information and Computer Sciences at the University of Hawaii. Surface synoptic reports were acquired in near real time via the Meteorology Department gopher server at The Florida State University. Brian Getzewich assisted with the data processing. We thank two anonymous reviewers for suggestions that led to significant improvements in the manuscript. This study was supported in part by NASA Grant NAGW-3944.

REFERENCES

Adler, R. F., G. J. Huffman, and P. R. Keehn, 1994: Global tropical rain estimates from microwave-adjusted geosynchronous IR data. *Remote Sens. Rev.*, **11,** 125–152.

Arkin, P. A., and B. N. Meisner, 1987: Spatial and annual variation in the diurnal cycle of large scale tropical convective cloudiness and precipitation. *Mon. Wea. Rev.*, **115,** 1009–1032.

——, and P. E. Ardanuy, 1989: Estimating climatic-scale precipitation from space: A review. *J. Climate*, **2,** 1229–1238.

——, R. Joyce, and J. E. Janowiak, 1994: The estimation of global monthly mean rainfall using infrared satellite data: The GOES Precipitation Index (GPI). *Remote Sens. Rev.*, **11,** 107–124.

Augustine, J. A., 1981: Insight into errors of SMS-inferred GATE convection rainfall. *J. Appl. Meteor.*, **20,** 509–520.

Battan, L. J., and R. R. Braham Jr., 1956: A study of convective precipitation based on cloud and radar observations. *J. Meteor.*, **13,** 587.

Bauer, P., and P. Schluessel, 1993: Rainfall, total water, ice water and water vapor over sea from polarized microwave simulations and SSM/I data. *J. Geophys. Res.*, **98,** 20 737–20 759.

Ferraro, R. R., F. Z. Weng, N. C. Grody, and A. Basist, 1996: An eight-year (1987–1994) time series of rainfall, clouds, water vapor, and sea ice derived from SSM/I measurements. *Bull. Amer. Meteor. Soc.*, **77,** 891–905.

Huffman, G. J., R. F. Adler, P. Arkin, A. Chang, R. Ferraro, A. Gruber, J. Janowiak, A. McNab, B. Rudolf, U. Schneider, 1997: The Global Precipitation Climatology Project (GPCP) combined precipitation dataset. *Bull. Amer. Meteor. Soc.*, **78,** 5–20.

Jaeger, L., 1983: Monthly and areal patterns of mean global precipitation. *Variations in the Global Water Budget*, A. Street-Perrott, M. Beran, and R. Ratcliffe, Eds., 129–140.

Janowiak, J. E., P. A. Arkin, P. Xie, M. L. Morrissey, and D. R. Legates, 1995: An examination of the east Pacific ITCZ rainfall distribution. *J. Climate*, **8,** 2810–2823.

Liu, G., and J. A. Curry, 1992: Retrieval of precipitation from satellite microwave measurements using both emission and scattering. *J. Geophys. Res.*, **97,** 9959–9974.

——, ——, and R.-S. Sheu, 1995: Classification of clouds over the western equatorial Pacific Ocean using combined infrared and microwave satellite data. *J. Geophys. Res.*, **100,** 13 811–13 826.

Petty, G. W., 1994a: Physical retrievals of over-ocean rain rate from multichannel microwave imagery. Part I: Theoretical characteristics of normalized polarization and scattering indices. *Meteor. Atmos. Phys.*, **54,** 79–100.

——, 1994b: Physical retrievals of over-ocean rain rate from mul-

tichannel microwave imagery. Part II: Algorithm implementation. *Meteor. Atmos. Phys.,* **54,** 101–122.
——, 1995a: The status of satellite-based rainfall estimation over land. *Remote Sens. Environ.* **51,** 125–137.
——, 1995b: Frequencies and characteristics of global oceanic precipitation from shipboard present-weather reports. *Bull. Amer. Meteor. Soc.,* **76,** 1593–1616.
——, 1997: An intercomparison of oceanic precipitation frequencies from 10 SSM/I rain rate algorithms and shipboard present-weather reports. *J. Geophys. Res.,* **102,** 1757–1777.
——, and W. Krajewski, 1996: Satellite rainfall estimation over land. *Hydrol. Sci. J.,* **41,** 433–451.
Simpson, J., C. Kummerow, W.-K. Tao, and R. F. Adler, 1996: On the Tropical Rainfall Measuring Mission (TRMM). *Meteor. Atmos. Phys.,* **60,** 19–36.
Sui, C.-H., K.-M. Lau, Y. N. Takayabu, and D. A. Short, 1997: Diurnal variations in tropical oceanic cumulus convection during TOGA COARE. *J. Atmos. Sci.,* **54,** 639–655.
Szoke, E. J., and E. J. Zipser, 1986: Radar study of convective cells in mesoscale systems in GATE. Part II: Life cycles of convective cells. *J. Atmos. Sci.,* **43,** 199–218.
Takahashi, N., and H. Uyeda, 1995: Doppler radar observation of the structure and characteristics of tropical clouds during the TOGA-COARE IOP in Manus, Papua New Guinea: Three case studies on November 23 and December 16, 1992. *J. Meteor. Soc. Japan,* **73,** 427–442.
Wilheit, T., A. Chang, and L. Chiu, 1991: Retrieval of monthly rainfall indices from microwave radiometric measurements using probability distribution function. *J. Atmos. Oceanic Technol.,* **8,** 118–136.
Williams, C. R., W. L. Ecklund, and K. S. Gage, 1995: *J. Atmos. Oceanic Technol.,* **12,** 996–1012.
Woodley, W. L., 1980: Inference of GATE convective rainfall from SMS-1 imagery. *J. Appl. Meteor.,* **19,** 388–408.
Xie, P., and P. A. Arkin, 1996: Analyses of global monthly precipitation using gauge observations, satellite estimates and numerical model predictions. *J. Climate,* **9,** 840–858.